

Meson loops in the Nambu–Jona-Lasinio model

Emil N. Nikolov^a, Wojciech Broniowski^b, Christo V. Christov^a,
Georges Ripka^c, and Klaus Goeke^a

^a *Institut für Theoretische Physik II, Ruhr-Universität Bochum,
D-44780 Bochum, Germany*

^b *H. Niewodniczański Institute of Nuclear Physics, PL-31342 Cracow, Poland*

^c *Service de Physique Théorique, Centre d'Etudes de Saclay, F-91191
Gif-sur-Yvette Cedex, France*



Ruhr-Universität Bochum
Institut für Theoretische Physik II
Teilchen- und Kernphysik

Meson loops in the Nambu-Jona-Lasinio model

Emil N. Nikolov ^{a,1}, Wojciech Broniowski ^b,
Christo V. Christov ^{a,1}, Georges Ripka ^c, and Klaus Goeke ^a

^a*Institut für Theoretische Physik II, Ruhr-Universität Bochum,
D-44780 Bochum, Germany*

^b*H. Niewodniczański Institute of Nuclear Physics, PL-31342 Cracow, Poland*

^c*Service de Physique Théorique de Saclay, F-91191 Gif-sur-Yvette Cedex, France*

Abstract

The effects of meson loops in the vacuum sector of the Nambu–Jona-Lasinio model are calculated. Using the effective action formalism we take consistently all next-to-leading-order $\frac{1}{N_c}$ terms into account. This leads to a symmetry-conserving approach, in which all features of spontaneously broken chiral symmetry, such as the Goldstone theorem, the Goldberger–Treiman and the Gell-Mann–Oakes–Renner relations are preserved. Contributions to $\langle \bar{q}q \rangle$ and F_π are calculated, and are shown to be substantial, at the level of $\sim 30\%$, consistent with the $\frac{1}{N_c}$ expansion. The leading nonanalytic terms in the chiral expansion of $\langle \bar{q}q \rangle$, F_π and m_π have the same form as the one-loop results of chiral perturbation theory.

PACS numbers: 12.39.-x, 12.39.Fe, 14.40.-n

1 Introduction

Over the last few years the Nambu–Jona-Lasinio model [1] has been used extensively to study numerous features of strong-interaction physics at low energies (for recent reviews on mesons see [2–4], and on baryons see [5,6]). The four-fermion point interaction leads to dynamical chiral symmetry breaking which plays a key role for the description of low-energy hadron phenomena. An attractive feature of the model is that having a small number of free

¹ On leave of absence from Institute for Nuclear Research and Nuclear Energy, 1784 Sofia, Bulgaria

² E-mail: emiln or christoc or goeke@hadron.tp2.ruhr-uni-bochum.de
broniowski@solaris.ifj.edu.pl
ripka@amoco.saclay.cea.fr

parameters it allows for a unified description of mesons and baryons, with both two and three flavors. The resulting hadron spectroscopy has been quite successful: the basic mass relations, the electromagnetic form factors and the electromagnetic polarizabilities are reproduced reasonably well.

All the above applications have been performed in the *one-quark-loop* approximation. The effective action, the meson and quark self-energies, vertex functions, *etc.*, are all generated by a quark-loop. This approximation is justified by the large- N_c limit, where meson loops are $\frac{1}{N_c}$ -suppressed. However, meson loops cannot always be neglected since in the real world $N_c = 3$. More importantly, the pions are very light, and in many situations pionic effects, although formally $\frac{1}{N_c}$ -suppressed, are enhanced because of the low pion mass. For example, pionic thermal excitations described by meson loops are dominating in hadronic systems at finite temperature. Meson loops are also required for the proper description of heavier mesons. For example, the σ or the ρ mesons can split into two pions and this effect is again described by pionic loops [7,8].

There have been a number of attempts [9–12] to include meson loops in the Nambu–Jona-Lasinio model. These approaches are based on $\frac{1}{N_c}$ expansion in terms of Feynman graphs. The symmetry properties of the system, however, can be easily violated by an inappropriate choice of diagrams. This is the case of Refs. [9–11] where basic symmetry relations, such as *e.g.* the Goldstone theorem, are violated. The reason for this is that the equation determining the expectation value of the σ field and expressions for the meson propagators are not consistent. We show that in order to guarantee the validity of the Goldstone theorem on the basis of a consistent $\frac{1}{N_c}$ expansion it is crucial to determine both the expectation value of the σ field and the meson propagators consistently, *e.g.* using the effective action including one-meson-loop contributions. Many-body methods which preserve the symmetry properties of the theory are called *symmetry-conserving approximations* [13,14]. The approach of Ref. [12] is up to our knowledge the only one which preserves the Goldstone theorem at the one meson-loop level. This is achieved by a judicious choice of Feynman diagrams.

In this paper we extend consistently the Nambu–Jona-Lasinio model to next-to-leading order in $\frac{1}{N_c}$ which includes the meson-loop contributions. We use the effective action formalism which leads in a natural way to a symmetry conserving approximation. Our approach identifies the Feynman diagrams which need to be included to maintain the symmetry properties, at any level of approximation. In our calculation the pion remains massless in the chiral limit and the basic relations following from Ward-Takahashi identities, such as the Gell-Mann–Oaks–Renner relation and the Goldberger-Treiman relation are satisfied. Furthermore, the leading nonanalytic terms in the chiral expansion of $\langle \bar{q}q \rangle$, F_π and m_π have the correct form, as given by chiral perturbation theory at the one-loop level [15].

We calculate numerically the contributions of meson loops to $\langle \bar{q}q \rangle$ and F_π , and find them to be substantial, of the order of 30%. This is consistent with the N_c -counting scheme.

The outline of the paper is as follows: In Sec. 2 we recall the model, establish the basic notation and review the formalism of the effective action. We

then proceed to evaluate the effective action at the quark-loop level (Sec. 3) and at the meson-loop level (Sec. 4), and derive expressions for the quark condensate (Sec. 5), the meson propagators (Sec. 6), and the pion decay constant (Sec. 7) at the one-meson-loop level. In Sec. 8 we verify explicitly that our expressions have the correct chiral expansion. Section Sec. 9 presents our numerical results. Appendices contain technical details of our calculation.

2 The effective action

We use the simplest version of the $SU(2)$ Nambu–Jona-Lasinio model [1] with scalar and pseudoscalar couplings only. The Lagrangian of the model is given by

$$\mathcal{L} = \bar{q}(i\partial^\mu\gamma_\mu - m)q + \frac{1}{2a^2} \left((\bar{q}q)^2 + (\bar{q}i\gamma_5\boldsymbol{\tau}q)^2 \right), \quad (1)$$

where the point-like four-quark interaction is characterized by the coupling constant $1/a^2$ with the dimension of inverse energy squared, q stands for up and down quarks with $N_c = 3$ colors, and m is the current quark mass. The partition function of the system is given by the path integral

$$Z = e^{-W} = \int \mathcal{D}q^\dagger \mathcal{D}q e^{-\mathcal{I}(q^\dagger, q)}. \quad (2)$$

The integration is over the Grassmann variables q^\dagger and q , and $\mathcal{I}(q^\dagger, q)$ is the Euclidean action

$$\mathcal{I}(q^\dagger, q) = \int d^4x q^\dagger (\partial_\tau - i\boldsymbol{\alpha} \cdot \boldsymbol{\nabla} + \beta m) q - \frac{1}{2a^2} \left((q^\dagger \beta q)^2 + (q^\dagger i\beta \gamma_5 \boldsymbol{\tau} q)^2 \right). \quad (3)$$

The partially bosonized version of the model [16] is obtained by introducing auxiliary meson fields Φ :

$$Z = \int \mathcal{D}q^\dagger \mathcal{D}q \mathcal{D}\Phi \exp \left\{ - \int d^4x \left[q^\dagger (\partial_\tau - i\boldsymbol{\alpha} \cdot \boldsymbol{\nabla} + \beta \Gamma_\alpha \Phi_\alpha) q + \frac{1}{2} a^2 \Phi^2 - a^2 m \Phi_0 + \frac{1}{2} a^2 m^2 \right] \right\}, \quad (4)$$

where we use the following notation

$$\begin{aligned} \Gamma_0 &= 1; & \Gamma_\alpha &= i\gamma_5 \tau_\alpha, \\ \Phi_0 &= S; & \Phi_\alpha &= P_\alpha, \quad \alpha = 1, 2, 3. \end{aligned} \quad (5)$$

The quark fields, which appear in the exponent of Eq. (4) in a quadratic form, can be integrated out, and the partition function becomes

$$Z \equiv e^{-W} = \int \mathcal{D}\Phi e^{-I(\Phi)}, \quad (6)$$

where $\int \mathcal{D}\Phi \equiv \int \mathcal{D}S \mathcal{D}\mathbf{P}$. The so called *bosonized* Euclidean action $I(\Phi)$ is given by

$$I(\Phi) = -N_c \text{Tr} \ln D + \int d^4x \left(\frac{a^2}{2} \Phi^2 - a^2 m \Phi_0 + \frac{a^2}{2} m^2 \right). \quad (7)$$

where we use the Dirac operator in the form

$$D = \partial_\tau + h \quad (8)$$

with the one-particle Dirac Hamiltonian h given by

$$h = -i\boldsymbol{\alpha} \cdot \boldsymbol{\nabla} + \beta \Gamma_\alpha \Phi_\alpha. \quad (9)$$

The trace in Eq. (7) involves an integration over space-time variables and a matrix trace over the spin and flavor degrees of freedom. The trace over color gives a factor N_c which we write explicitly. Recalling that the quark propagator in the background meson fields Φ is given by D^{-1} , we refer to the term $N_c \text{Tr} \ln D$ as to the *quark-loop contribution*.

For simplicity we use the following notation throughout the paper: the indices a, b, \dots contain the field isospin indices α, β, \dots and the space-time coordinates x_a, x_b, \dots , *i.e.* $a \equiv \{\alpha, x_a\}$, $b \equiv \{\beta, x_b\}$, *etc.* Summation/integration over repeated indices is understood.

Generally, the quark-loop contribution $N_c \text{Tr} \ln D$ can have an imaginary part which is related to the *anomalous* terms. In the case of SU(2) with scalar and pseudoscalar mesons this imaginary part vanishes identically and the one-quark-loop contribution is given by the real part: $N_c \text{Tr} \ln D = \frac{1}{2} N_c \text{Tr} \ln(D^\dagger D)$ such that the Euclidean action can also be written in the form

$$I(\Phi) = -\frac{1}{2} N_c \text{Tr} \ln(D^\dagger D) + \int d^4x \left(\frac{a^2}{2} \Phi^2 - a^2 m \Phi_0 + \frac{a^2}{2} m^2 \right). \quad (10)$$

and $D^\dagger D$ can be written in the covariant form

$$D^\dagger D = \partial_\mu \partial_\mu + i\gamma_\mu \Gamma_\alpha (\partial_\mu \Phi_\alpha) + \Phi^2. \quad (11)$$

The bosonized action $I(\Phi)$ is a functional of the fields $\Phi_\alpha(x)$. The effective action in the one-meson-loop approximation is given by [17,18]:

$$\Gamma(\Phi) = I(\Phi) + \frac{1}{2} \text{Tr} \ln \frac{\delta^2 I(\Phi)}{\delta \Phi \delta \Phi}. \quad (12)$$

The effective action (12) has the following properties [18,14]:

- At the stationary point of the action, the values of the fields Φ_a represent the ground-state expectation values of the field operators.
- The inverse field propagators L^{-1} are equal to the second order derivatives of the effective action:

$$L_{ab}^{-1} = \frac{\delta^2 \Gamma(\Phi)}{\delta \Phi_a \delta \Phi_b}, \quad (13)$$

calculated at the stationary point. The same result can be deduced by a resummation of Feynman graphs, in terms of quark propagators which are dressed by a general static potential [14,19]. We refer to the action $I(\Phi)$, which is leading order in N_c , as the one-quark-loop approximation, and to the effective action (12), including both the leading and next to leading order term $\frac{1}{2} \text{Tr} \ln \frac{\delta^2 I(\Phi)}{\delta \Phi \delta \Phi}$, as the one-meson-loop approximation. We emphasize that in our approach they are both symmetry conserving approximations.

Most applications of the Nambu Jona-Lasinio model so far, have neglected the contribution of the second term (the meson loop contribution) to the action (12). The purpose of this paper is to include this contribution in the description of the vacuum and the pion properties.

3 The regularized effective action in the one-quark-loop approximation

We first consider the one-quark-loop approximation, in which the second term of the effective action (10) is neglected. In this approximation

$$\Gamma(\Phi) = I(\Phi) = -\frac{N_c}{2} \text{Tr} \ln(D^\dagger D) + \int d^4x \left(\frac{a^2}{2} \Phi^2 - a^2 m \Phi_0 + \frac{a^2}{2} m^2 \right). \quad (14)$$

The effective action (14) is ultraviolet divergent and requires regularization. To this aim a fermion-loop cut-off Λ_f is introduced. Since the model is non-renormalizable, the cut-off Λ_f is kept finite and treated as a parameter.

In this paper we use two regularization schemes, namely the proper-time regularization and the covariant four-momentum $O(4)$ regularization, as used in Ref. [20]. We will compare results obtained with these schemes. The proper-time regularized effective action is given by

$$I_{\Lambda}(\Phi) = \frac{N_c}{2} \text{Tr} \int_{\Lambda_f^{-2}}^{\infty} \frac{ds}{s} e^{-sD^{\dagger}D} + \int d^4x \left(\frac{a^2}{2} \Phi^2 - a^2 m \Phi_0 + \frac{a^2}{2} m^2 \right). \quad (15)$$

In the $O(4)$ regularization, the four-momentum running in the quark loop is limited by $|k| < \Lambda_f$ as explained in App. B.2. In the following we will always use the regularized action and skip the index Λ . The action (15) has a translationally invariant stationary point at $\Phi = (M_0, 0, 0, 0)$

$$\left. \frac{\delta I(\Phi)}{\delta \Phi_a} \right|_{M_0} = 0. \quad (16)$$

The stationary point M_0 is identified with the vacuum expectation value of the S field in the one quark-loop approximation. Inserting the regularized effective action (15) into Eq. (16) we get the following equation for M_0 :

$$a^2 \left(1 - \frac{m}{M_0} \right) - 8N_c g(M_0) = 0, \quad (17)$$

where the function g is defined in App. B. Equation (17) is commonly referred to as the gap equation since it determines the energy gap $2M_0$ between the negative- and positive-energy quark states. Obviously, M_0 plays the role of the *constituent* mass of the quark.

In the one-quark-loop approximation, the inverse meson propagators (13) are given by the second variation of the action with respect to the fields, taken *at the stationary point* $(M_0, 0, 0, 0)$:

$$K_{ab}^{-1} = \left. \frac{\delta^2 I(\Phi)}{\delta \Phi_a \delta \Phi_b} \right|_{M_0}. \quad (18)$$

In momentum space the inverse meson propagators are given by [20]

$$K_{\alpha\beta}^{-1}(q^2) = \delta_{\alpha\beta} \left\{ 4N_c \left(f(M_0, q^2)(q^2 + 4M_0^2 \delta_{\alpha 0}) - 2g(M_0) \right) + a^2 \right\}, \quad (19)$$

where the function f describing a quark loop with two meson couplings is given in App. B. Since we are evaluating the propagator at the stationary point $(M_0, 0, 0, 0)$, we can use the gap equation (17) in order to simplify this expression and obtain the pseudoscalar and scalar inverse meson propagators in the form

$$K_{\pi}^{-1}(q^2) = 4N_c f(M_0, q^2) q^2 + a^2 \frac{m}{M_0}, \quad (20)$$

$$K_{\sigma}^{-1}(q^2) = 4N_c f(M_0, q^2)(q^2 + 4M_0^2) + a^2 \frac{m}{M_0}. \quad (21)$$

The propagators have poles at

$$m_\pi^2 = \frac{a^2 m}{4N_c f(M_0, q^2 = -m_\pi^2) M_0} , \quad (22)$$

$$m_\sigma^2 = 4M_0^2 + \frac{a^2 m}{4N_c f(M_0, q^2 = -m_\sigma^2) M_0} , \quad (23)$$

where m_π and m_σ are the on-shell pion and σ -meson masses. In the chiral limit ($m \rightarrow 0$), the pseudoscalar mesons are massless Goldstone bosons, as expected. The physical quark-meson coupling constant $g_{\pi qq}$ is given by the residue at the pole of the pion propagator

$$g_{\pi qq}^2 = \lim_{q^2 \rightarrow -m_\pi^2} (q^2 + m_\pi^2) K_\pi(q^2), \quad (24)$$

which gives in the chiral limit

$$g_{\pi qq} = (4N_c f(M_0, 0))^{-\frac{1}{2}} . \quad (25)$$

To end this section we recall the N_c -counting rules for quark and meson loops in the Nambu–Jona-Lasinio model. From the gap equation (17) it follows that the coupling constant $\frac{1}{a^2}$ must be considered proportional to $\frac{1}{N_c}$. Each quark-loop contributes a factor of N_c , which comes from the trace over color degrees of freedom. Thus, the action $I(\Phi)$ is of order N_c . The meson propagators contain a quark-loop in the denominator and are hence of order $\frac{1}{N_c}$, as can be seen directly from Eq. (19). From Eq. (25) we find that the physical pion-quark coupling constant $g_{\pi qq}$ is of order $N_c^{-\frac{1}{2}}$. The physical pion field ($\boldsymbol{\pi} = \boldsymbol{P}/g_{\pi qq}$) is obtained by rescaling the meson field \boldsymbol{P} . The propagator for the physical pion field has the form $K_\pi(q^2)/g_{\pi qq}^2$, which is of order N_c^0 . For each quark–physical pion vertex we have a factor of $g_{\pi qq} \sim N_c^{-\frac{1}{2}}$. Analogous relations hold for the sigma field. This way, N_c -counting rules in the NJL model agree with those of QCD [21,22].

4 The regularized effective action including the meson-loop contribution

In this section we include the meson-loop contribution to the effective potential, which is the second term of the expression (12). This leads to corrections which are next-to-leading order in N_c . We now consider the effective action in the form (12)

$$\Gamma(\Phi) = I(\Phi) + \frac{1}{2} \text{Tr} \ln K^{-1}(\Phi) , \quad (26)$$

where $K^{-1}(\Phi)$ is the functional

$$K_{ab}^{-1} = \frac{\delta^2 I(\Phi)}{\delta \Phi_a \delta \Phi_b}. \quad (27)$$

Evaluating the meson-loop term, $\frac{1}{2} \text{Tr} \ln K^{-1}(\Phi)$, we encounter new divergences which arise due to the integration over the momentum in the meson-loop. Let us analyze the meson-loop momentum integrals from a formal point of view. In our model, which has only quark dynamical degrees of freedom, the meson propagator at the leading N_c -level is given by a chain of quark-loops. We have regularized the quark-loop contribution introducing a fermionic cut-off parameter Λ_f . This regularization, however, does not restrict the four-momenta of the mesons. Using the asymptotics of the function f at high momenta it can be easily shown that the leading order field propagator has the asymptotic expansion $K_{\alpha\beta}^{-1}(q^2) \underset{q^2 \rightarrow \infty}{\approx} \delta_{\alpha\beta} a^2 + \mathcal{O}\left(\frac{1}{q^2}\right)$. Thus, integrating over the meson-loop four-momentum in (26) we encounter a quartic divergence. Similarly, calculating the pion propagator at the one-meson-loop level we will obtain both quadratically and logarithmically divergent terms. We regularize the meson-loop integrals introducing a new *bosonic* cut-off parameter Λ_b . We use a covariant $O(4)$ regularization for the meson loop, consisting in cutting off the meson four-momenta in the loop integrals at $Q^2 = \Lambda_b^2$. This is the simplest possible choice.

The one-meson-loop effective action (26) has a translationally invariant stationary point $\Phi = (M, 0, 0, 0)$ given by the equation

$$\left. \frac{\delta \Gamma(\Phi)}{\delta \Phi_a} \right|_M = 0. \quad (28)$$

The stationary point of the one-meson-loop effective action Γ is denoted by M , in order to distinguish it from the stationary point M_0 of the quark-loop action defined in Eq. (16).

We note that M *does not* correspond to the pole of the quark propagator at the one-meson-loop level — it is not the quark mass. It is only the local (Hartree) contribution to the quark propagator mass. The quantity M is the expectation value of the S field when meson-loop effects included. We may rewrite Eq. (28) in the form

$$\left. \frac{\delta \Gamma(\Phi)}{\delta \Phi_a} \right|_M = S_a(M) + \frac{1}{2} S_{abc}(M) K_{bc}(M) = 0, \quad (29)$$

where we have introduced the following short-hand notation for the n -leg quark-loop meson vertices

$$S_{a_1 a_2 \dots a_n}(M) \equiv \left. \frac{\delta^n I(\Phi)}{\delta \Phi_{a_1} \delta \Phi_{a_2} \dots \delta \Phi_{a_n}} \right|_M. \quad (30)$$

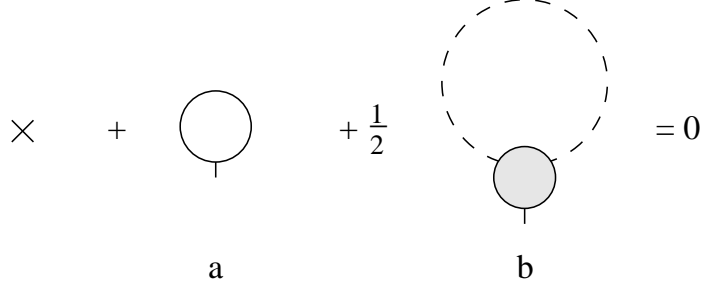


Fig. 1. Diagrammatic representation of Eq. (31): (a) the quark-loop contribution, (b) the meson-loop contribution. The cross denotes the constant term $a^2(1 - m/M)$. The short external lines denote the scalar-isoscalar coupling, the solid line in (a) denotes the (regularized) quark propagator, the dashed line in (b) denotes the meson propagator \widetilde{K} defined in Eq. 33, and the filled blob denotes the meson vertex S_{0bc} , explicitly given in App. A.

For $a = 1, 2, 3$, the condition (29) is trivially satisfied with a vanishing pion field. From the variation over the sigma field we obtain

$$S_0(M) + \frac{1}{2}S_{0bc}(M)K_{bc}(M) = 0. \quad (31)$$

We represent Eq. (31) digrammatically in Fig. 1. The first two terms where present at the quark-loop level. The cross is the contact term contribution to $S_0(M)$, and (a) denotes the quark-loop contribution. The term (b) is the meson-loop contribution. The meaning of symbols is explained in the caption. Using the N_c -counting rules (see Section 3) it can be verified that the meson-loop diagram (b) is of order N_c^0 and hence suppressed by one power in $\frac{1}{N_c}$ compared to the quark-loop diagram, which is of order N_c . The leading-order meson propagators in Eq. (31) $K_{bc}(M)$ are evaluated at the stationary point of the one-meson-loop effective action, M . In momentum space, similarly to Eq. (19), we obtain

$$\begin{aligned} K_{\alpha\beta}^{-1}(M, q^2) &= \delta_{\alpha\beta} \left\{ 4N_c \left(f(M, q^2)(q^2 + 4M^2\delta_{\alpha 0}) - 2g(M) \right) + a^2 \right\} \\ &= \widetilde{K}_{\alpha\beta}^{-1}(M, q^2) + \delta_{\alpha\beta}\Delta(M), \end{aligned} \quad (32)$$

where we have defined

$$\widetilde{K}_{\alpha\beta}^{-1}(M, q^2) = \delta_{\alpha\beta} \left[4N_c f(M, q^2)(q^2 + 4M^2\delta_{\alpha 0}) + \frac{a^2 m}{M} \right] \quad (33)$$

and

$$\Delta(M) = -8N_c g(M) + a^2 \left(1 - \frac{m}{M} \right). \quad (34)$$

Since $\Delta(M)$ is exactly equal to the first term $S_0(M)$ in Eq. (31) we have

$$\Delta(M) = S_0(M) = -\frac{1}{2}S_{0bc}(M)K_{bc}(M) = \mathcal{O}(N_c^0), \quad (35)$$

which shows that $\Delta(M)$ is one order in N_c suppressed compared to the full propagators (32) which are of order N_c . Inserting the decomposition (32) into Eq. (31) we obtain

$$S_0(M) + \frac{1}{2}S_{0bc}(M)\widetilde{K}_{bc}(M) - \frac{1}{2}S_{0bc}(M)\widetilde{K}_{bd}(M)S_0(M)\widetilde{K}_{dc}(M) + \dots = 0. \quad (36)$$

The third term in this expansion is of order $\frac{1}{N_c}$ and hence one order in N_c suppressed compared to the meson-loop contribution (the second term). Further terms are suppressed by even higher powers of N_c . At the present level of approximation we should therefore keep only the first two terms in Eq. (36) — otherwise consistency in N_c -counting is lost.

The explicit form of Eq. (36) used in numerical calculations has the form

$$\begin{aligned} & a^2 \left(1 - \frac{m}{M}\right) - 8N_c g(M) + \frac{N_c}{4\pi^4} \int d^4Q \times \\ & \left\{ \left[2f(M, 0) + \frac{d}{dM^2} \left(f(M, Q^2)(Q^2 + M^2) \right) \right] \widetilde{K}_\sigma(M, Q^2) \right. \\ & \left. + 3 \left[2f(M, 0) + \frac{d}{dM^2} f(M, Q^2)Q^2 \right] \widetilde{K}_\pi(M, Q^2) \right\} = 0, \end{aligned} \quad (37)$$

5 Quark condensate

The quark condensate $\langle \bar{q}q \rangle$ is given by $\langle \bar{q}q \rangle = \delta\Gamma(\Phi)/\delta m$ which from Eq. (26) immediately gives

$$\langle \bar{q}q \rangle = -a^2(M - m). \quad (38)$$

Comparing the result (38) with the corresponding expression at the one-quark-loop level, $\langle \bar{q}q \rangle = -a^2(M_0 - m)$, we can see that it is analogous, with M_0 replaced by M . We shall compare our theoretical results to the empirical value [23]

$$\langle \bar{u}u \rangle = \langle \bar{d}d \rangle = \frac{1}{2} \langle \bar{q}q \rangle = -((250 \pm 50) \text{ MeV})^3. \quad (39)$$

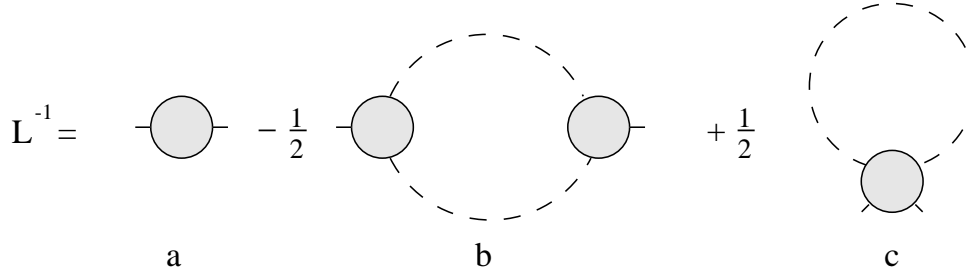


Fig. 2. Diagrams contributing to the inverse meson propagator in one-meson-loop approximation: (a) quark-loop contribution, (b–c) meson-loop contributions. The dashed line denotes the meson propagator \tilde{K} , and the filled quark-loop meson vertices are defined in App. A.

6 Meson propagators

The inverse meson propagators, including the one-meson-loop effects, are equal to the second order variation (13) of the effective action (26) with respect to the fields taken at the stationary point M :

$$L_{ab}^{-1} = \left. \frac{\delta^2 \Gamma(\Phi)}{\delta \Phi_a \delta \Phi_b} \right|_M. \quad (40)$$

Performing the variation in (40) we can express the propagators in one-meson-loop approximation in terms of the functional K (27) and the quark-loop meson vertices (30):

$$L_{ab}^{-1} = K_{ab}^{-1}(M) - \frac{1}{2} S_{ace}(M) K_{cd}(M) K_{ef}(M) S_{dfb}(M) + \frac{1}{2} S_{abcd}(M) K_{cd}(M). \quad (41)$$

The diagrammatic representation of this equation is shown in Fig. 2. The first term is the leading-order (quark-loop) contribution $K^{-1}(M)$. We have to bare in mind, however, that here it differs from the inverse propagator $K^{-1}(M_0)$ in the one-quark-loop approximation, because it is evaluated at the new stationary point M of the one-meson-loop effective action. This means that the quark propagators appearing in the meson propagator $K(M)$ are dressed by solving Eq.(36). The second (b) and third term (c) are the one-meson-loop contributions to the inverse meson propagator. The dashed lines in the loops correspond to a pion or to a sigma meson. The one-meson-loop contributions are suppressed one order in N_c , which can be easily shown using the N_c -counting rules.

In Eq. (41) M is the solution of the Eq. (36), in which only the first two terms are retained, so as to be consistent with N_c -counting. It is crucial to maintain

the same N_c -counting consistency in the calculation of the meson propagators (41). We include in the inverse propagator L^{-1} contributions which are of order N_c and N_c^0 . In the first term K^{-1} , which is defined in Eq. (32), we keep both the contributions \widetilde{K}^{-1} , of order N_c , and the contribution $\Delta(M)$, of order N_c^0 . In the remaining (meson-loop) terms of Eq. (41), the vertices S are of order N_c (because they contain a quark loop) and the leading order of the K operators is N_c^{-1} . Therefore N_c -counting consistency requires the substitution of K with \widetilde{K} in the two meson-loop terms. Keeping all terms to order N_c^0 we obtain the inverse meson propagators in the form

$$L_{ab}^{-1} = K_{ab}^{-1}(M) - \frac{1}{2}S_{ace}(M)\widetilde{K}_{cd}(M)\widetilde{K}_{ef}(M)S_{dfb}(M) + \frac{1}{2}S_{abcd}(M)\widetilde{K}_{cd}(M), \quad (42)$$

where the propagators \widetilde{K}_{ab} in the meson loops are given by (33).

Despite the simple form (42) of inverse meson propagators, their numerical evaluation for an arbitrary momentum is quite involved. It requires integration over the meson-loop four-momentum Q , over the momenta in the quark-loops as well as over the proper-time (or Feynman) parameters. Even after taking some of the integrals analytically we still end up with many-dimensional integrals that must be evaluated numerically. However, we are first of all interested in pionic properties. Since the pion is very light, we can determine the pion mass and the pion-quark coupling constant from the low-momentum expansion of the pion propagator. This leads to a radical simplification of the numerical calculation. The inverse pion propagator in momentum space can be expanded in the form

$$L_{\pi}^{-1}(q^2) = L_{\pi}^{-1}(0) + Z_{\pi}(0)q^2 + \mathcal{O}(q^4). \quad (43)$$

Both the constant term, $L_{\pi}^{-1}(0)$, and the q^2 -term, $Z_{\pi}(0)$, can be expressed as a sum of three contributions corresponding to the diagrams in Fig. 2.

We will now check that the pion remains massless when the $\frac{1}{N_c}$ meson-loop corrections are taken into account. It is crucial for the proof that the expectation value of the S field, M , is determined from the stationary-point condition for the effective action. We note that at the one-meson-loop level the stationary point of the effective action and the quark self energy do not coincide. In the approaches of Refs. [9–11] where the gap equation at the one-meson-loop level includes the quark self-energy diagram the Goldstone theorem does not hold. It does hold in the work of Ref. [12], where the quark self energy diagram has been replaced by a tadpole diagram. Thus contributions of the same order in N_c as the calculated meson-loop correction have been excluded in order to fulfill the Goldstone theorem. The retained tadpole diagram is exactly the one obtained by dressing the quark propagator by a general static potential and hence in the approach of Ref. [12] one can recognize a symmetry conserving approximation [14].

In order to check the validity of the Goldstone theorem we have to evaluate the leading-order term $L_\pi^{-1}(0)$ in the low-momentum expansion of the inverse pion propagator. We write the inverse pion propagator at zero momentum as a sum of the contributions of the three diagrams in Fig. 2, in which we have now couplings with zero external pion momentum. This leads to a significant simplification in the evaluation of the diagrams. The algebra is straightforward but tedious, and we refer the reader to Ref. [24] for details. The result is

$$\begin{aligned}
L_\pi^{-1}(0) = & a^2 - 8N_c g(M) + \frac{N_c}{4\pi^4} \int d^4Q \times \\
& \left\{ \left[2f(M, 0) + \frac{d}{dM^2} \left(f(M, Q^2)(Q^2 + M^2) \right) \right] \widetilde{K}_\sigma(M, Q^2) \right. \\
& \left. + 3 \left[2f(M, 0) + \frac{d}{dM^2} f(M, Q^2) Q^2 \right] \widetilde{K}_\pi(M, Q^2) \right\} , \tag{44}
\end{aligned}$$

Using Eq. (37) in (44) we obtain immediately

$$L_\pi^{-1}(0) = a^2 \frac{m}{M}, \tag{45}$$

which is analogous to the one-quark-loop result with M_0 replaced with M . In the chiral limit ($m = 0$) we have $L_\pi^{-1}(0) = 0$, showing that the pions are massless. Thus, as expected, the Goldstone theorem is satisfied in the one meson-loop approximation. This is a general feature. If we derive both the gap equation and the meson propagators by performing functional derivatives of the effective action, we have a symmetry-conserving approximation. The Goldstone pion reflects this.

For non-vanishing quark current mass m the chiral symmetry is explicitly broken and the pion acquires a finite mass. It is given by the position of the pole of the pion propagator. Using the inverse pion propagator we obtain

$$L_\pi^{-1}(-m_\pi^2) = L_\pi^{-1}(0) - Z_\pi(-m_\pi^2) m_\pi^2 = 0 \tag{46}$$

and using Eq. (45) we obtain the on-shell pion mass as a solution of the following equation

$$m_\pi^2 = \frac{a^2 m}{Z_\pi(-m_\pi^2) M}. \tag{47}$$

Since m_π is very small we can approximate $Z_\pi(-m_\pi^2)$ by its value at zero momentum. Then we can calculate the pion mass in one meson-loop approximation using the results for the low-momentum expansion of the pion propagator

$$m_\pi^2 = \frac{a^2 m}{Z_\pi(0) M} + \mathcal{O}(m_\pi^4). \tag{48}$$

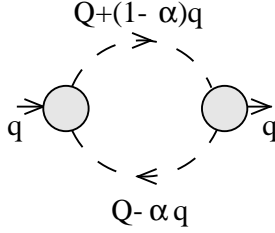


Fig. 3. The routing ambiguity in the meson-loop contributions of Fig. 2, diagram (b), to the inverse pion propagator.

The pion-quark coupling constant can be determined on the one-meson-loop level similarly to (24) as the residue of the pion propagator at its pole

$$g_{\pi qq}^2 = \lim_{q^2 \rightarrow -m_\pi^2} (q^2 + m_\pi^2) L_\pi^{-1}(q^2). \quad (49)$$

In the chiral limit we obtain the simple result

$$g_{\pi qq} = (Z_\pi(0))^{-\frac{1}{2}}. \quad (50)$$

In order to evaluate m_π and $g_{\pi qq}$ we need, in addition to M which we obtain by solving Eq. (36), the wave-function renormalization $Z_\pi(0)$. The steps in this calculation are as follows: We expand various contributions of Fig. 2 in powers of the external momentum q and isolate the coefficient of q^2 . The momentum in loops is cut by the mesonic cut-off Λ_b . In the case of diagram (b) we have, for this cut-off prescription, an ambiguity in routing the momentum in the loop, as shown in Fig. 3. Depending on the value of the routing parameter α , we get different numerical results. In this paper we average with equal weights over all α from 0 to 1. This prescription is arbitrary, and one could use another one, *e.g.* choose $\alpha = \frac{1}{2}$. As we will see, the choice of routing does not affect fundamental properties, such as GMOR relation, or the form of the leading nonanalytic terms in the chiral expansion (see Sec. 8). Obviously, it does affect the numerical value of m_π and F_π to some extent. The algebra and final expressions for $Z_\pi(0)$ are lengthy, and the reader is referred to Ref. [24] for details.

7 The pion decay constant

The pion decay constant is an important quantity in our calculations, since we use its empirical value in order to fix the parameters of the model. Its evaluation allows us also to check explicitly the Goldberger-Treiman relation for the quarks, which gives the connection between M , the pion-quark cou-

pling constant in the chiral limit. The Gell-Mann–Oakes–Renner relation then follows straightforwardly.

The pion decay constant F_π is defined by the matrix element for the weak pion decay

$$\langle 0 | A_\mu^\alpha(z) | \pi^\beta(q) \rangle = -i\delta^{\alpha\beta} q_\mu F_\pi e^{-iq \cdot z}, \quad (51)$$

where $A_\mu^\alpha = \bar{q}\gamma_\mu\gamma_5\tau^\alpha/2q$ is the axial current and $\boldsymbol{\pi}$ is the physical pion field $\boldsymbol{\pi} = \mathbf{P}/g_{\pi qq}$. Applying the Lehmann-Symanzik-Zimmermann reduction formula we can relate the pion decay constant $F_\pi = F(-m_\pi^2)$ to the form factor $F(q^2)$, which can be expressed in terms of the expectation value of the time-ordered product

$$\langle 0 | T[A_\mu^\alpha(z), \pi^\beta(0)] | 0 \rangle = -i\delta^{\alpha\beta} \int \frac{d^4q}{(2\pi)^4} F(q^2) \frac{q_\mu}{q^2 + m_\pi^2} e^{-iq \cdot z}. \quad (52)$$

To evaluate this matrix element we couple an external axial source j_μ^α in the effective action, which gives for the Dirac operator (*cf.* Eq. (8))

$$D = \beta \left(-i\gamma_\mu \partial_\mu + \Gamma_\beta \Phi_\beta + \gamma^\mu \gamma_5 \frac{\tau_\alpha}{2} j_\mu^\alpha \right). \quad (53)$$

Inserting this operator in the action we obtain the generating functional in the presence of the source j_μ^α for the external axial field. Then the matrix element (52) can be expressed as a variation of the generating functional

$$\langle 0 | T[A_\mu^\alpha(z), \pi^\beta(0)] | 0 \rangle = \frac{1}{g_{\pi qq}} \int d^4x \frac{\delta^2 \Gamma}{\delta j_\mu^\alpha(z) \delta \pi^\beta(x)} \Big|_{j=0} L_\pi(x). \quad (54)$$

The rhs of this equation has the same structure as the one-meson-loop pion propagator (40) with one derivative with respect to the meson field replaced by a derivative with respect to the axial source. Hence, in the one-meson-loop approximation, we obtain contributions to the pion decay constant from diagrams analogous to those contributing to the inverse meson propagators (Fig. 2), but with one of the external meson couplings replaced by an axial coupling.

We calculate F_π from the low-momentum expansion as we did for the one meson-loop pion propagator, with the same routing prescription. The difference is that now we pick up the terms linear in the external momentum q_μ . Also, due to the axial coupling, we obtain different spin-isospin structure of the quark-loop functions. The calculation is straightforward but tedious, and details are in Ref. [24]. The final result is

$$F_\pi = g_{\pi qq} M Z_\pi(m_\pi^2). \quad (55)$$

In the chiral limit this reduces to the Goldberger-Treiman relation [25] for the quarks

$$g_{\pi qq} F_\pi = M. \quad (56)$$

Using this result and the expressions for the pion mass (48) and the quark condensate (38) at the one-meson-loop level we recover also the Gell-Mann–Oakes–Renner relation [26]:

$$m \langle \bar{q}q \rangle = -m_\pi^2 F_\pi^2 + \mathcal{O}(m_\pi^4). \quad (57)$$

We have shown that in our effective action approach the Goldstone theorem, the Goldberger-Treiman, and the Gell-Mann–Oakes–Renner relations are valid with the meson loops included. Thus the basic relations following from Ward-Takahashi identities are satisfied in the one-meson-loop approximation. Again, this is a feature of a symmetry-conserving approximation.

8 Chiral expansions

In this section we check that the leading nonanalytic terms in chiral expansion of the quark condensate, the pion mass and the pion decay constant agree with the one-loop results of chiral perturbation theory.

In chiral perturbation theory [15] we have

$$\langle \bar{q}q \rangle = \langle \bar{q}q \rangle_0 \left(1 - \frac{3m_\pi^2}{32\pi^2 F_\pi^2} \log m_\pi^2 + \dots \right), \quad (58)$$

where $\langle \bar{q}q \rangle_0$ is the value of the quark condensate in the chiral limit. We wish to show the same result holds in the NJL model with meson loops. Equation (37), which we may write as $G(M, m) = 0$, defines M as an implicit function of m . We have therefore

$$\frac{dM}{dm} = -\frac{\frac{\partial G}{\partial m}}{\frac{\partial G}{\partial M}}. \quad (59)$$

We find explicitly

$$\frac{\partial G}{\partial M} = a^2 m / M^2 - 8N_c dg(M)/dM + \mathcal{O}(N_c^0) = \frac{4M}{g_{\pi qq}^2} + \mathcal{O}(N_c^0) + \mathcal{O}(m), \quad (60)$$

where we have used the identity $dg(M)/dM = -2Mf(M, 0)$, and the relation (25). For $\frac{\partial G}{\partial m}$ the only infrared nonanalytic term is the pion-loop term, the last

one in Eq. (37). Close to the pion pole this piece is

$$3N_c \frac{1}{4\pi^2} \int_0^{\Lambda_b} d(Q^2) Q^2 \frac{2f(M, 0)}{4N_c f(M, 0) Q^2 + a^2 m/M}, \quad (61)$$

which yields the nonanalytic term $\frac{3}{8\pi^2} m_\pi^2 \log(m_\pi^2/\Lambda^2)$ via Eq. (48). From (60) and (59) we find immediately

$$\frac{dM}{dm_\pi^2} = -\frac{3g_{\pi qq}^2}{32\pi^2 M} \frac{d}{dm_\pi^2} \left(m_\pi^2 \log(m_\pi^2/\Lambda^2) \right) + \mathcal{O}(1/N_c^2) + \mathcal{O}(m_\pi^2). \quad (62)$$

Using Eq. (56) in (62) we get

$$M = M_{m=0} \left(1 - \frac{3m_\pi^2}{32\pi^2 F_\pi^2} \log m_\pi^2 + \dots \right), \quad (63)$$

where $M_{m=0}$ is the value of M in the chiral limit. From the fact that $\langle \bar{q}q \rangle = -a^2(M - m)$ we immediately establish the desired result (58). Note, that for m_π and F_π in the above expression we use the leading- N_c pieces. The subleading pieces to these quantities are relevant in relative $1/N_c^2$ corrections to $\langle \bar{q}q \rangle$, which is not considered at the present level of approximation.

Chiral perturbation theory also determines the leading nonanalytic terms in the expansion of m_π and F_π . Denoting the leading- N_c values of the pion mass and decay constant by $m_{\pi,0}$ and $F_{\pi,0}$ (in the notation of Ref. [15] these are M and F — the tree-level pion mass and decay constant), we have

$$m_\pi^2 = m_{\pi,0}^2 \left(1 + \frac{m_{\pi,0}^2}{32\pi^2 F_{\pi,0}^2} \log m_{\pi,0}^2 + \dots \right) \quad (64)$$

$$F_\pi = F_{\pi,0} \left(1 - \frac{m_{\pi,0}^2}{16\pi^2 F_{\pi,0}^2} \log m_{\pi,0}^2 + \dots \right). \quad (65)$$

In order to check that these expansions hold in our treatment of the NJL model, we first look at the chiral expansion of $Z_\pi(0)$. There are cancellations occuring between the quark and meson loop contributions, and the final answer is

$$Z_\pi(0) = Z_{\pi,0}(0) \left(1 + \frac{m_{\pi,0}^2}{16\pi^2 F_{\pi,0}^2} \log m_{\pi,0}^2 + \dots \right). \quad (66)$$

The above result is independent of the routing ambiguity of Fig. 3. Using expansions (63) and (66) in Eqs. (48) and (56) we obtain the desired expressions (64-65).

We emphasize that the agreement of the results of this section with chiral perturbation theory is a direct consequence of the symmetry-conserving approximation.

We have also performed a numerical study in order to check how good is expansion (58) in our case. For typical parameters ($a = 162\text{MeV}$, $\Lambda_f = \Lambda_b = 755\text{MeV}$, $m = 0$) we find that $\langle\bar{q}q\rangle = -(173.8\text{MeV})^3$, and for same parameter but $m = 13\text{MeV}$, which fits the pion mass to its physical value, we have $\langle\bar{q}q\rangle = -(175.0\text{MeV})^3$, *i.e.* a 5% change. In comparison, Eq. (58) would give 8% with the chiral scale under the log taken to be 1GeV. This shows that the leading nonanalytic correction accounts for a major part of the change of the condensate as one departs from the chiral limit.

9 Numerical results and discussion

At the one-quark-loop level the model has the following parameters: the quark-quark coupling constant $\frac{1}{a^2}$, the quark cut-off Λ_f , and the current quark mass m . With the meson loop included we have in addition the meson cut-off Λ_b . We use the empirical values for the observables in the meson sector, namely $F_\pi = 93\text{ MeV}$, and $m_\pi = 139\text{ MeV}$ in order to fix the model parameters. After fitting the pion mass and decay constant, we are left with two free parameters. We could fix one of them by fitting the phenomenological value of the quark condensate $\langle\bar{q}q\rangle$. The results of our calculation for $\langle\bar{q}q\rangle$, however, are quite sensitive to the cut-off procedure. Furthermore, the experimental range for $\langle\bar{q}q\rangle$ is very wide, $(-\frac{1}{2}\langle\bar{q}q\rangle)_{\text{exp}}^{\frac{1}{3}} = 250 \pm 50\text{ MeV}$. For these reasons we do not use the value of the quark condensate to fix the parameters. Since we do not know the particular physics underlying the regularization of the theory, QCD cannot be a guide to fix the loop cut-offs Λ_f and Λ_b . In this exploratory calculation we display results obtained for four values of the ratio $\Lambda_b/\Lambda_f = 0, 0.5, 1$, and 1.5 . Using the gap equation we eliminate the coupling constant $1/a^2$ in favor M , which we treat as a free parameter. Thus all quantities are presented as a function of M for different values of the ratio Λ_b/Λ_f .

We present the calculations performed in the chiral limit ($m = 0$). Introducing a nonzero current quark mass m leads to small corrections to the calculated quantities. Since at this point we are mainly interested in the general behavior of the quark condensate as a function of the model parameters we find it useful to start by considering the chiral limit. The quantity M in one-meson-loop approximation is given by the solution of Eq. (31). We use this equation in order to determine the fermionic cut-off Λ_f for given values of M and Λ_b/Λ_f . We plot Λ_f as a function of M for different values of the ratio Λ_b/Λ_f of the bosonic to the fermionic cut-off. The results in the chiral limit ($m = 0$) with proper-time and $O(4)$ fermion-loop regularization are presented in Figs. 4 and 5, respectively. The pion decay constant F_π is fitted to reproduce the experimental value. For $\Lambda_b = 0$ we recover the results of the one-quark-loop approximation, so that the difference between the lowest curve and the other curves is a measure of the meson loop contribution. For Λ_f lower than a critical value we do not have spontaneous breaking of the chiral symmetry and Eq. (17) has no solution. With increasing mesonic cut-off Λ_b the critical value of Λ_f increases

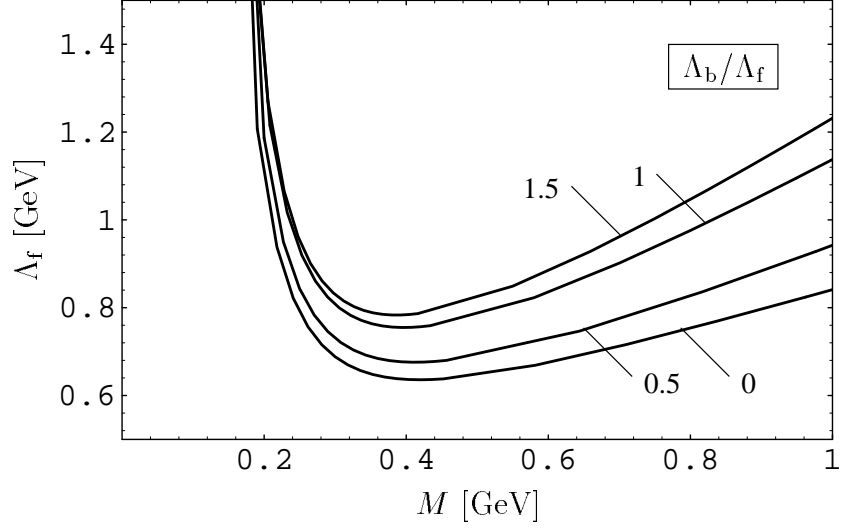


Fig. 4. The fermionic cut-off Λ_f for proper-time quark-loop regularization as a function of M for different values of Λ_b/Λ_f . The curves correspond to $\Lambda_b/\Lambda_f = 0, 0.5, 1, 1.5$.

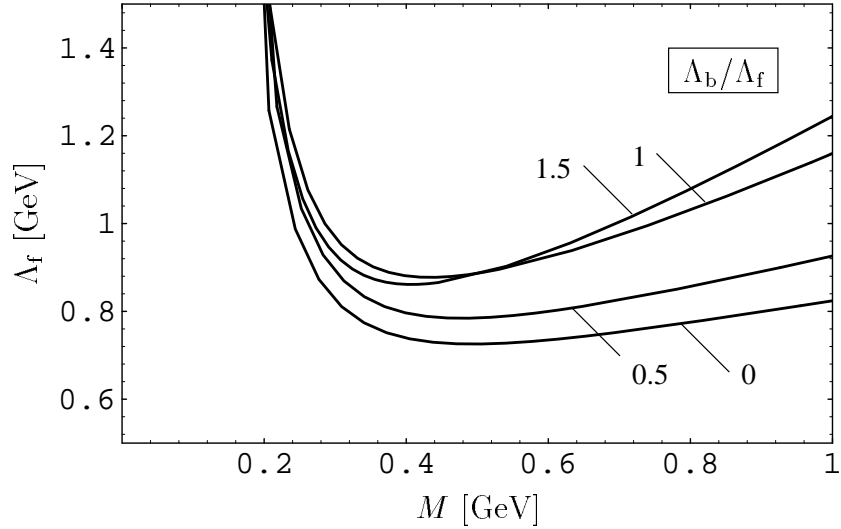


Fig. 5. The fermionic cut-off Λ_f for $O(4)$ quark-loop regularization as a function of M for different values of Λ_b/Λ_f . The curves correspond to $\Lambda_b/\Lambda_f = 0, 0.5, 1, 1.5$. Note that the curve for $\Lambda_b/\Lambda_f = 1.5$ has the critical Λ_f smaller than for $\Lambda_b/\Lambda_f = 1$.

and the curve “moves” up until Λ_b/Λ_f reaches ~ 1.5 for the proper-time cut-off and ~ 1.2 for the $O(4)$ one. For larger values of Λ_b/Λ_f the minimal value of Λ_f starts decreasing and the curve moves down with increasing Λ_b/Λ_f . This differs from the results of Dmitrašinović *et al.* [12] with Pauli-Villars fermion-loop regularization where the curves keep moving towards larger values of Λ_f as Λ_b/Λ_f increases (see Fig. 11 in [12]). For large mesonic cut-offs, Λ_b/Λ_f over 2 for the proper-time fermion regularization and Λ_b/Λ_f over 3 in the $O(4)$ case, we do not have solution of Eq. (36) with F_π fitted to the experimental

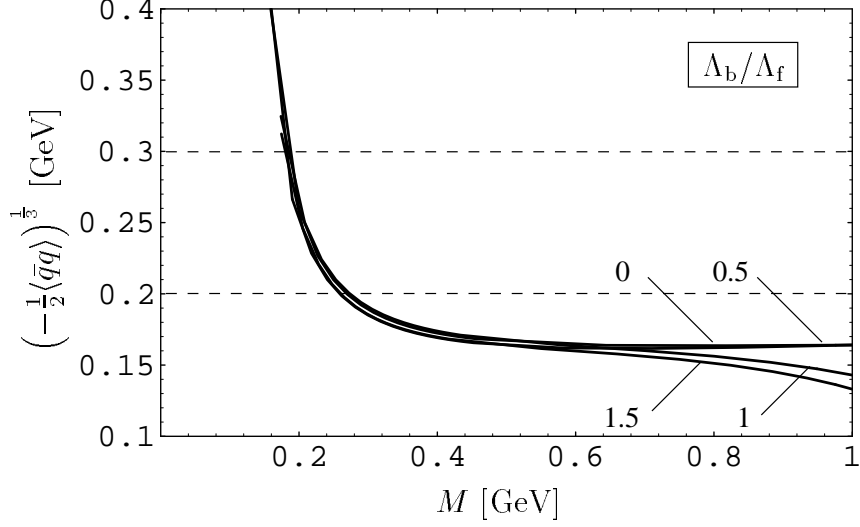


Fig. 6. The quark condensate $\left(-\frac{1}{2}\langle\bar{q}q\rangle\right)^{\frac{1}{3}}$ with proper-time quark-loop regularization as a function of M for different values of Λ_b/Λ_f . The curves correspond to $\Lambda_b/\Lambda_f = 0, 0.5, 1, 1.5$. The dashed lines mark the empirical bounds.

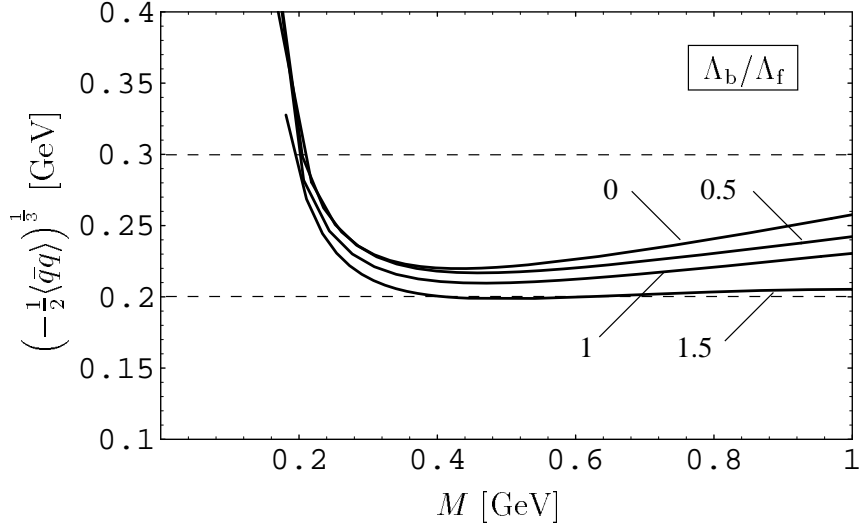


Fig. 7. The quark condensate $\left(-\frac{1}{2}\langle\bar{q}q\rangle\right)^{\frac{1}{3}}$ with $O(4)$ quark-loop regularization as a function of M for different values of Λ_b/Λ_f . The curves correspond to $\Lambda_b/\Lambda_f = 0, 0.5, 1.5, 1$. The dashed lines mark the empirical bounds.

value. Calculations in the baryon sector of the Nambu–Jona-Lasinio model with one quark and zero boson loops [27,28] show that best results for baryonic properties are obtained for M in the range 400–500 MeV, *i.e.* for values of the quark cut-off near the critical value. Although this picture may change when meson-loop effects are included, we note that the value M for the critical value of the quark cut-off changes very little. For $\Lambda_b \sim \Lambda_f$ the fermion cut-off increases by about 30%.

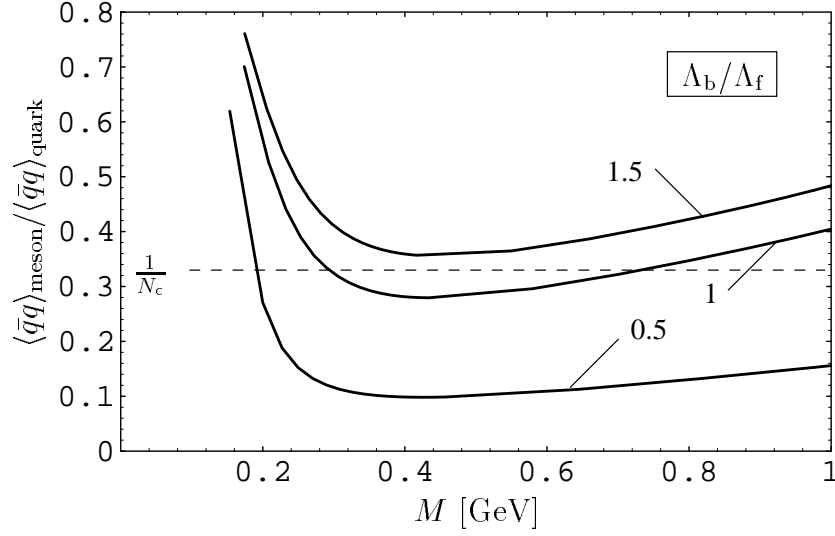


Fig. 8. The ratio of the meson-loop to the quark-loop contribution to $\langle \bar{q}q \rangle$ as a function of M obtained with proper-time fermion-loop regularization. The curves correspond to $\Lambda_b/\Lambda_f = 0.5, 1, 1.5$.

Comparing the results of the two fermion-loop regularization procedures we can see that although the critical values of Λ_f , below which there is no spontaneous chiral symmetry breaking are quite different, the general behavior of M as a function of the fermionic and mesonic cut-offs is very similar.

The quark condensate is given in terms of M and the quark-quark coupling constant by Eq. (38). The results in the chiral limit are shown in Figs. 6 and 7 for the proper-time and $O(4)$ fermion-loop regularizations. They are plotted as a function of M for the four different ratios Λ_b/Λ_f . The empirical value for the quark condensate is obtained in chiral perturbation theory using the value of the quark current mass (Gell-Mann–Oakes–Renner relation) [29] or from QCD sum-rules. The phenomenological uncertainty (39) is, however, quite wide. With both the proper-time and $O(4)$ cut-offs there is a plateau for M between 0.3 and 0.6 GeV and the corresponding value of $\langle \bar{q}q \rangle$ depends little on Λ_b/Λ_f . The value in the proper-time case (Fig. 6) is underestimated. This problem is known from the one-quark-loop calculations, where better agreement can be obtained using a generalized two-parameter proper-time regularization function. In the case of the $O(4)$ quark-loop regularization (Fig. 7) our results for the quark condensate are in the phenomenological bounds for values of M in the plateau region. This shows that the quark condensate is sensitive to the particular quark-loop regularization procedure, a feature well known from the calculations in the one-quark-loop approximation.

In Fig. 8 we plot the ratio of the meson-loop to the quark-loop contribution to $\langle \bar{q}q \rangle$ as a function of M for the proper-time quark-loop regularization. The relative contribution of the meson loop increases with increasing Λ_b/Λ_f . For values of the parameters in the range $0.3 < M < 0.6$ GeV and $\Lambda_b/\Lambda_f < 1$ we have $\langle \bar{q}q \rangle_{\text{meson}} / \langle \bar{q}q \rangle_{\text{quark}} < 40\%$, *i.e.* of the order of $\frac{1}{N_c}$ as expected.

Looking at Figs. 6 and 8 we see that as Λ_b/Λ_f increases the meson-loop con-

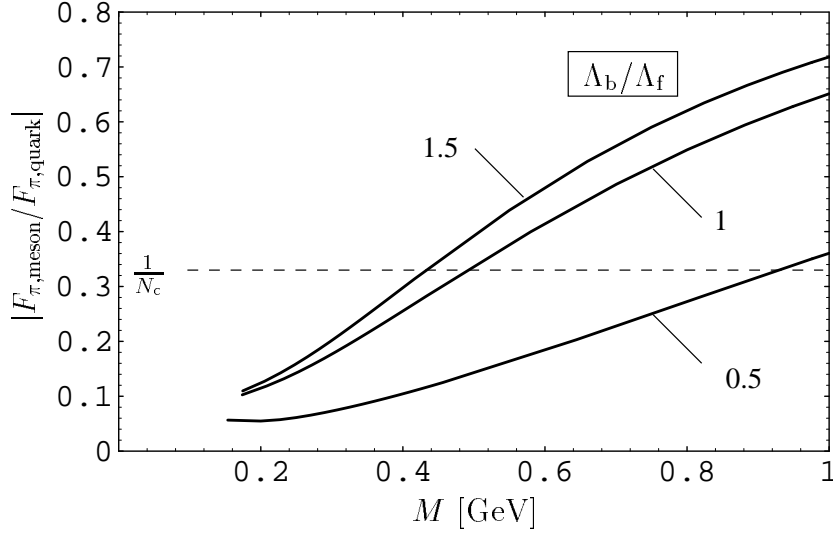


Fig. 9. The ratio of the meson-loop to the quark-loop contribution to F_π as a function of M obtained with proper-time fermion-loop regularization. The curves correspond to $\Lambda_b/\Lambda_f = 0.5, 1, 1.5$.

tribution to the quark condensate increases, while the quark-loop contribution decreases. The sum of the contributions remains roughly constant. Eq. (38) shows that the inclusion of the meson-loops does not significantly change the four-quark coupling constant $\frac{1}{a^2}$.

Let us now come back to the N_c -counting scheme, which we extensively used throughout the meson-loop calculations presented above. We have calculated the meson-loop corrections to the quark condensate, the pion mass and the pion decay constant, showing that they are one order in N_c suppressed. However, the expansion in powers of $\frac{1}{N_c}$ should be used with care since $N_c = 3$. Furthermore, the meson-loop corrections depend on the mesonic cut-off Λ_b and are infinite for $\Lambda_b \rightarrow \infty$. Hence it is important to check how well does the N_c -counting scheme work for the particular values of the parameters.

In the previous section we have compared the meson-loop and quark-loop contributions to $\langle \bar{q}q \rangle$ and found that for reasonable values of the parameters the ratio $\langle \bar{q}q \rangle_{\text{meson}} / \langle \bar{q}q \rangle_{\text{quark}}$ is in the expected range. Here we compare the meson- and quark-loop contributions to F_π . Since we have fixed the parameters in order to reproduce the experimental value of the pion decay constant the sum of both contributions gives $F_{\pi,\text{quark}} + F_{\pi,\text{meson}} = 93 \text{ MeV}$, but their relative contributions depend on the choice of parameters. The meson-loop contribution is negative. In Fig. 9 we show the ratio $|F_{\pi,\text{meson}}/F_{\pi,\text{quark}}|$ with proper-time quark-loop regularization. The relative contribution of the meson-loop grows with increasing M . It is larger for larger values of Λ_b/Λ_f . As we mentioned in the previous section, the empirical value of F_π can be only reproduced for Λ_b/Λ_f less than about 2, which sets an upper bound for the meson-loop cut-off. For values of Λ_b in this range and $M < 0.6 \text{ GeV}$ the meson-loop correction does not exceed 40% of the N_c -leading quark-loop term. This is important because it keeps the $\frac{1}{N_c}$ corrections in the expected range. It justifies *a posteriori* the use of the N_c -counting scheme. The above observations are also

true for the quark condensate (see Fig. 8) as well as for the $O(4)$ fermionic regularization. In the case when $\Lambda_b \simeq \Lambda_f$ and $0.3 < M < 0.6$ MeV we find that the meson-loop contributions are of the order of $\frac{1}{N_c} = \frac{1}{3}$ compared to the leading-order contributions.

10 Conclusion

We have shown that the effective action formalism in the Nambu–Jona-Lasinio model leads to a symmetry-conserving approximation, allowing us include consistently meson-loop effects while preserving the usual properties associated with spontaneous chiral symmetry breaking (the Goldstone theorem, the Gell-Mann–Oaks–Renner relation, the form of the leading nonanalytic terms in the chiral expansion of various quantities). Indeed, meson-loop effects will destroy these properties unless both the gap equation and meson propagators are treated consistently. This has already been noticed in Ref. [12], where Feynman diagrams were used. In our approach the conservation of the symmetry properties is a natural consequence of the consistent application of the $\frac{1}{N_c}$ expansion. We have found that though meson-loop contributions are $\frac{1}{N_c}$ -suppressed as compared to the leading-order quark-loop contributions they lead to substantial corrections. For the physically reasonable values of the model parameters the effects of meson loops to the pion decay constant and to the quark condensate are of the expected order of 30%.

Acknowledgment

The authors acknowledge the support of the Volkswagen Foundation (EN, CC), the Bulgarian National Science Foundation, contract Φ -406 (EN, CC), of the Polish State Committee of Scientific Research, grant 2 P03B 188 09 (WB), and of the Alexander von Humboldt Foundation (GR, WB), as well as partial support by COSY, BMBF, PROCOPE, and Stiftung für Deutsch-Polnische Zusammenarbeit.

A Quark-loop meson vertices

In our meson-loop calculations we need the meson vertices which couple different number of mesons (we need up to four) through a quark loop. They are given by the variations of the effective action with respect to the meson fields. To obtain these we first expand the action in powers of the meson field fluctuations around the stationary point. We perform the expansion for the proper-time regularized effective action. Using the proper-time expressions we can easily obtain the four-momentum regularized expressions as well.

We start from the proper-time regularized effective action

$$I = \frac{N_c}{2} \text{Tr} \int_{\Lambda_f^{-2}}^{\infty} \frac{ds}{s} e^{-sD^\dagger D} + \frac{a^2}{2} \Phi^2 - a^2 m \Phi_0, \quad (\text{A.1})$$

where $D^\dagger D$ is given by

$$D^\dagger D = \partial_\mu \partial_\mu + i\gamma_\mu \Gamma_\alpha (\partial_\mu \Phi_\alpha) + \Phi^2. \quad (\text{A.2})$$

The fields Φ are now fluctuating around the stationary-point constant fields which are of the form $\Phi^{\text{st}} = \{S, 0, 0, 0\}$

$$\Phi = \Phi^{\text{st}} + \delta\Phi. \quad (\text{A.3})$$

Expanding $D^\dagger D$ in terms of the meson field fluctuations we obtain

$$D^\dagger D \equiv G_0^{-1} + V, \quad (\text{A.4})$$

where

$$G_0^{-1} = \partial^\mu \partial_\mu + \Phi^{\text{st}2} \quad (\text{A.5})$$

is the zero-order term in $\delta\Phi$ which is diagonal in momentum space and the fluctuation term is given by

$$\begin{aligned} V &= V^{(1)} + V^{(2)}, \\ V^{(1)} &= 2\Phi_a^{\text{st}} \delta\Phi_a + i\gamma_\mu \Gamma_\alpha (\partial_\mu \delta\Phi_\alpha), \\ V^{(2)} &= (\delta\Phi)^2 \end{aligned} \quad (\text{A.6})$$

and consists of terms of first, $V^{(1)}$, and second order, $V^{(2)}$, in the field fluctuations. Next we expand the exponent in the fermionic part of the effective action (A.1) in powers of V using the Feynman-Schwinger-Dyson formula and the cyclic property of the trace

$$\begin{aligned} I_f &= \frac{N_c}{2} \text{Tr} \int_{\Lambda_f^{-2}}^{\infty} \frac{ds}{s} \left(e^{-sD^\dagger D} \right) \\ &= \frac{N_c}{2} \text{Tr} \int_{\Lambda_f^{-2}}^{\infty} \frac{ds}{s} \left\{ e^{-sG_0^{-1}} - sV e^{-sG_0^{-1}} + \frac{s^2}{2} \int_0^1 du V e^{-s(1-u)G_0^{-1}} V e^{-suG_0^{-1}} \right. \end{aligned}$$

$$\begin{aligned}
& -\frac{s^3}{3} \int_0^1 du \int_0^{1-u} dv V e^{-s(1-u-v)G_0^{-1}} V e^{-suG_0^{-1}} V e^{-svG_0^{-1}} \\
& + \frac{s^4}{4} \int_0^1 du \int_0^{1-u} dv \int_0^{1-u-v} dw V e^{-s(1-u-v-w)G_0^{-1}} V e^{-suG_0^{-1}} V e^{-svG_0^{-1}} V e^{-swG_0^{-1}} \Big\}
\end{aligned} \tag{A.7}$$

The first term in this expansion (zero order in V) gives the quark contribution to the one-quark-loop effective action (15). The term linear in $\delta\Phi$ cancels with the mesonic terms in the expansion of the action since we expand around the stationary point.

The term quadratic in $\delta\Phi$ acquires contributions from the linear and quadratic in V terms as well as from the mesonic part of the effective action. Evaluating it in momentum space and taking the second variation with respect to the meson fields we obtain

$$\begin{aligned}
S_{ab} & \equiv \frac{\delta^2 I}{\delta\Phi_\alpha(q_1)\delta\Phi_\beta(q_2)} \\
& = \delta_{\alpha\beta}\delta(q_1 + q_2) \left\{ 4N_c \left[f(S, q_1)(q_1^2 + 4S^2\delta_{\alpha 0}) - 2g(S) \right] + a^2 \right\}, \tag{A.8}
\end{aligned}$$

where the functions f and g are calculated in App. B.

The third order term in the expansion of the action I in powers of the field fluctuations $\delta\Phi$ acquires contributions from the second and third order in V terms in (A.7)

$$I^{(3)} = I^{(3A)} + I^{(3B)}, \tag{A.9}$$

$$I^{(3A)} = N_c \sum_{C_V} \text{Tr} \int_{\Lambda_f^{-2}}^\infty ds \frac{s}{4} \int_0^1 du V^{(1)} e^{-s(1-u)G_0^{-1}} V^{(2)} e^{-suG_0^{-1}}, \tag{A.10}$$

$$\begin{aligned}
I^{(3B)} & = -N_c \text{Tr} \int_{\Lambda_f^{-2}}^\infty ds \frac{s^2}{6} \int_0^1 du \int_0^{1-u} dv V^{(1)} e^{-s(1-u-v)G_0^{-1}} \\
& \quad \times V^{(1)} e^{-suG_0^{-1}} V^{(1)} e^{-svG_0^{-1}},
\end{aligned} \tag{A.11}$$

where \sum_{C_V} denotes the sum over the permutations of $V^{(1)}$ and $V^{(2)}$. Varying this expressions with respect to the meson fields we obtain the corresponding three-leg quark-meson vertex functions in momentum space

$$S_{abc}^{(A)} \equiv \frac{\delta^3 I^{(3A)}}{\delta\Phi_\alpha(q_1)\delta\Phi_\beta(q_2)\delta\Phi_\gamma(q_3)} = 8N_c \sum_P \delta(q_1 + q_2 + q_3) \Phi_\alpha^{\text{st}} \delta_{\beta\gamma}$$

$$\times \int_{\Lambda_f^{-2}}^{\infty} ds s \int_0^1 du \int \frac{d^4 k}{(2\pi)^4} e^{-s(1-u)((k+q_1)^2+S^2)} e^{-su(k^2+S^2)}, \quad (\text{A.12})$$

$$\begin{aligned} S_{abc}^{(B)} &\equiv \frac{\delta^3 I^{(3B)}}{\delta\Phi_\alpha(q_1)\delta\Phi_\beta(q_2)\delta\Phi_\gamma(q_3)} = -\frac{8N_c}{3} \sum_P^{3!} \delta(q_1 + q_2 + q_3) \\ &\times \left(4\Phi_\alpha^{\text{st}}\Phi_\beta^{\text{st}}\Phi_\gamma^{\text{st}} + \delta_{\alpha\beta}\Phi_\gamma^{\text{st}} q_1 \cdot q_2 + \delta_{\beta\gamma}\Phi_\alpha^{\text{st}} q_2 \cdot q_3 + \delta_{\alpha\gamma}\Phi_\beta^{\text{st}} q_1 \cdot q_3 \right) \\ &\times \int_{\Lambda_f^{-2}}^{\infty} ds s^2 \int_0^1 du \int_0^{1-u} dv \int \frac{d^4 k}{(2\pi)^4} \\ &\times e^{-s(1-u-v)((k+q_1)^2+S^2)} e^{-su((k+q_1+q_2)^2+S^2)} e^{-sv(k^2+S^2)}, \end{aligned} \quad (\text{A.13})$$

where we have introduced the notation \sum_P for the sum over the permutations of the couples of meson-field indices and momenta $\{(\alpha, q_1), (\beta, q_2), (\gamma, q_3), \dots\}$. Summing the two contributions we obtain finally

$$S_{abc} = S_{abc}^{(A)} + S_{abc}^{(B)}. \quad (\text{A.14})$$

The fourth order term in the expansion of I in powers of the field fluctuations $\delta\Phi$ acquires contributions from the second, third and fourth order in V terms in (A.7)

$$I^{(4)} = I^{(4A)} + I^{(4B)} + I^{(4C)}, \quad (\text{A.15})$$

$$I^{(4A)} = N_c \text{Tr} \int_{\Lambda_f^{-2}}^{\infty} ds \frac{s}{4} \int_0^1 du V^{(2)} e^{-s(1-u)G_0^{-1}} V^{(2)} e^{-suG_0^{-1}}, \quad (\text{A.16})$$

$$\begin{aligned} I^{(4B)} &= -N_c \sum_{C_V}^3 \text{Tr} \int_{\Lambda_f^{-2}}^{\infty} ds \frac{s^2}{6} \int_0^1 du \int_0^{1-u} dv \\ &\times V^{(2)} e^{-s(1-u-v)G_0^{-1}} V^{(1)} e^{-suG_0^{-1}} V^{(1)} e^{-svG_0^{-1}}, \end{aligned} \quad (\text{A.17})$$

$$\begin{aligned} I^{(4C)} &= N_c \text{Tr} \int_{\Lambda_f^{-2}}^{\infty} ds \frac{s^3}{8} \int_0^1 du \int_0^{1-u} dv \int_0^{1-u-v} dw \\ &\times V^{(1)} e^{-s(1-u-v-w)G_0^{-1}} V^{(1)} e^{-suG_0^{-1}} V^{(1)} e^{-svG_0^{-1}} V^{(1)} e^{-swG_0^{-1}}. \end{aligned} \quad (\text{A.18})$$

We evaluate the traces in momentum space and vary with respect to the meson fields in order to obtain the corresponding contributions to the four-leg quark-meson vertex

$$S_{abcd}^{(A)} \equiv \frac{\delta^4 I^{(4A)}}{\delta \Phi_\alpha(q_1) \delta \Phi_\beta(q_2) \delta \Phi_\gamma(q_3) \delta \Phi_\delta(q_4)} = 2N_c \sum_P^{4!} \delta(q_1 + q_2 + q_3 + q_4) \\ \times \delta_{\alpha\beta} \delta_{\gamma\delta} \int_{\Lambda_f^{-2}}^{\infty} ds s \int_0^1 du \int \frac{d^4 k}{(2\pi)^4} e^{-s(1-u)((k+q_1+q_2)^2+S^2)} e^{-su(k^2+S^2)}, \quad (\text{A.19})$$

$$S_{abcd}^{(B)} \equiv \frac{\delta^4 I^{(4B)}}{\delta \Phi_\alpha(q_1) \delta \Phi_\beta(q_2) \delta \Phi_\gamma(q_3) \delta \Phi_\delta(q_4)} = -4N_c \sum_P^{4!} \delta(q_1 + q_2 + q_3 + q_4) \\ \times \delta_{\alpha\beta} \delta_{\gamma\delta} (q_3 \cdot q_4 + 4S^2 \delta_{\gamma 0}) \int_{\Lambda_f^{-2}}^{\infty} ds s^2 \int_0^1 du \int_0^{1-u} dv \int \frac{d^4 k}{(2\pi)^4} \\ \times e^{-s(1-u-v)((k+q_1+q_2)^2+S^2)} e^{-su((k+q_1+q_2+q_3)^2+S^2)} e^{-sv(k^2+S^2)}, \quad (\text{A.20})$$

$$S_{abcd}^{(C)} \equiv \frac{\delta^4 I_{\text{eff}}^{(4C)}}{\delta \Phi_\alpha(q_1) \delta \Phi_\beta(q_2) \delta \Phi_\gamma(q_3) \delta \Phi_\delta(q_4)} = N_c \sum_P^{4!} \delta(q_1 + q_2 + q_3 + q_4) \\ \times \left[16\Phi_\alpha^{\text{st}} \Phi_\beta^{\text{st}} \Phi_\gamma^{\text{st}} \Phi_\delta^{\text{st}} + 4 \sum_{C_{V'}}^6 (\delta_{\mu\nu} \Phi_\kappa^{\text{st}} \Phi_\chi^{\text{st}} q_i \cdot q_j) + (\delta^{\alpha\beta} \delta^{\gamma\delta} - \delta^{\alpha\gamma} \delta^{\beta\delta} + \delta^{\alpha\delta} \delta^{\beta\gamma}) \right. \\ \left. \times ((q_1 \cdot q_2)(q_3 \cdot q_4) - (q_1 \cdot q_3)(q_2 \cdot q_4) + (q_1 \cdot q_4)(q_2 \cdot q_3)) \right] \\ \times \int_{\Lambda_f^{-2}}^{\infty} ds s^3 \int_0^1 du \int_0^{1-u} dv \int_0^{1-u-v} dw \int \frac{d^4 k}{(2\pi)^4} e^{-s(1-u-v-w)((k+q_1)^2+S^2)} \\ \times e^{-su((k+q_1+q_2)^2+S^2)} e^{-sv((k+q_1+q_2+q_3)^2+S^2)} e^{-sw(k^2+S^2)}, \quad (\text{A.21})$$

where in the last contribution $\sum_{C_{V'}}^6$ stays for the sum over combinations, originating from different orderings of the two terms in $V^{(1)}$ (A.6)

$$\sum_{C_{V'}}^6 (\delta_{\mu\nu} \Phi_\kappa^{\text{st}} \Phi_\chi^{\text{st}} q_i \cdot q_j) \equiv \delta_{\alpha\beta} \Phi_\gamma^{\text{st}} \Phi_\delta^{\text{st}} q_1 \cdot q_2 + \delta_{\alpha\gamma} \Phi_\beta^{\text{st}} \Phi_\delta^{\text{st}} q_1 \cdot q_3 \\ + \delta_{\alpha\delta} \Phi_\beta^{\text{st}} \Phi_\gamma^{\text{st}} q_1 \cdot q_4 + \delta_{\beta\gamma} \Phi_\alpha^{\text{st}} \Phi_\delta^{\text{st}} q_2 \cdot q_3 + \delta_{\beta\delta} \Phi_\alpha^{\text{st}} \Phi_\gamma^{\text{st}} q_2 \cdot q_4 + \delta_{\gamma\delta} \Phi_\alpha^{\text{st}} \Phi_\beta^{\text{st}} q_3 \cdot q_4. \quad (\text{A.22})$$

Summing up all contributions we obtain finally

$$S_{abcd} = S_{abcd}^{(A)} + S_{abcd}^{(B)} + S_{abcd}^{(C)}. \quad (\text{A.23})$$

B Regularization functions

Here we calculate the regularization functions for the quark-loop vertices in the diagrams for the gap equation and pion propagator. We start by evaluating the regulators in the proper-time scheme. The $O(4)$ regulators can be then easily obtained using the intermediate results of the proper-time case.

B.1 Proper-time regularization

We start by evaluating the function g emerging in the one-quark-loop gap equation. It is given by

$$\begin{aligned} g(S) &\equiv \int \frac{d^4 k}{(2\pi)^4} \int_{\Lambda_f^{-2}}^{\infty} ds e^{-s(k^2+S^2)} \\ &= \frac{1}{16\pi^2} \left(\Lambda_f^2 e^{-\frac{S^2}{\Lambda_f^2}} - S^2 E_1 \left(\frac{S^2}{\Lambda_f^2} \right) \right), \end{aligned} \quad (\text{B.1})$$

where E_1 is the exponential integral defined by

$$E_n(x) \equiv \int_1^{\infty} dt \frac{e^{-xt}}{t^n}. \quad (\text{B.2})$$

The function f is defined by

$$\begin{aligned} f(S, q^2) &\equiv \int \frac{d^4 k}{(2\pi)^4} \int_{\Lambda_f^{-2}}^{\infty} ds s \int_0^1 du e^{-s(1-u)((k+\frac{q}{2})^2+S^2)} e^{-su((k-\frac{q}{2})^2+S^2)} \\ &= \frac{1}{16\pi^2} \int_0^1 du E_1 \left(\frac{S^2 + u(1-u)q^2}{\Lambda_f^2} \right). \end{aligned} \quad (\text{B.3})$$

B.2 $O(4)$ regularization

Here we define the quark-loop $O(4)$ regularization. The running four-momentum of the quark loop is limited in the following manner. We obtain the quark-loop vertex functions in our $O(4)$ regularization scheme using the intermediate results from the proper-time calculation. After having completed the square

for the fermion-loop four-momentum k in the proper-time expressions we take the limit in the *proper-time* fermionic cut-off $\Lambda_f^{PT} \rightarrow \infty$ using the identity

$$\lim_{\Lambda_f^{PT} \rightarrow \infty} \int_{(\Lambda_f^{PT})^{-2}}^{\infty} ds s^n e^{-sA} = \frac{n!}{A^{n+1}}, \quad \text{for } n \geq 0, A > 0. \quad (\text{B.4})$$

Then we cut off the integral at some $O(4)$ cut-off $\Lambda_f^{O(4)}$ and obtain the $O(4)$ regularization functions. Note that in the following expressions both the k^2 - and u -integrals can be taken analytically. This leads, however, to quite lengthy sums of logarithms and rational functions, and for the sake of clarity we present the regularization functions keeping the integrals.

The function $g(S)$ can be easily obtained from the $O(4)$ -regularized action

$$g(S) = \frac{1}{16\pi^2} \int_0^{\Lambda_f^2} d(k^2) \frac{k^2}{k^2 + S^2}, \quad (\text{B.5})$$

Using Eq. (B.3) we obtain

$$f(S, q^2) = \frac{1}{16\pi^2} \int_0^{\Lambda_f^2} d(k^2) \int_0^1 du \frac{k^2}{(k^2 + S^2 + u(1-u)q^2)^2}, \quad (\text{B.6})$$

References

- [1] Y. Nambu and G. Jona-Lasinio, Phys. Rev. **122** (1961) 345
- [2] W. Weise, Univ. of Regensburg preprint TPR-93-2
- [3] U. Vogl and W. Weise, Progr. Part. Nucl. Phys. **7** (1991) 195
- [4] J. Bijnens, Phys. Rep. **265** (1996) 369
- [5] R. Alkofer, H. Reinhardt, and H. Weigel, Phys. Rep. **265** (1996) 139
- [6] Chr. V. Christov *et al.*, Progress in Part. and Nucl. Physics **37** (1996) 1
- [7] S. Krewald, K. Nakayama, and J. Speth, Phys. Lett. **B272** (1991) 190
- [8] L. S. Celenza, A. Pantziris, C. M. Shakin, and J. Szweda, Phys. Rev. **C47** (1993) 2356
- [9] N.-W. Cao, C. M. Shakin, and W.-D. Sun, Phys. Rev. **C46** (1992) 2535
- [10] P. P. Domitrovich, D. Bückers, and H. Müther, Phys. Rev. **C48** (1993) 413

- [11] E. Quack and S. P. Klevansky, Phys. Rev. C49 (1994) 3283; P. Zhuang, J. Hüfner, and S. P. Klevansky, Nucl. Phys. A576 (1994) 525; P. Zhuang, J. Hüfner, S. P. Klevansky, and H. Voss, Ann. Phys. (N.Y.) 234 (1994) 225
- [12] V. Dmitrašinović, H.-J. Schulze, R. Tegen, and R. H. Lemmer, Ann. Phys. (N.Y.) **238** (1995) 332
- [13] L. P. Kadanoff and G. Baym, *Quantum Statistical Mechanics* (Benjamin, New York, 1962)
- [14] J.-P. Blaizot and G. Ripka, *Quantum Theory of Finite Systems* (MIT Press, Cambridge, 1986)
- [15] J. Gasser and H. Leutwyler, Ann. Phys. (N.Y.) **158** (1984) 142
- [16] T. Eguchi, Phys. Rev. D **14** (1975) 2755
- [17] S. Coleman and E. Weinberg, Phys. Rev. **D7** (1973) 1888
- [18] C. Itzykson and J.-B. Zuber, *Quantum Field Theory* (McGraw-Hill, New York, 1980)
- [19] R. Padjen and G. Ripka, Nucl. Phys. **A149** (1970) 273
- [20] M. Jaminon, R. M. Galain, G. Ripka, and P. Stassart, Nucl. Phys. **A537** (1992) 418
- [21] G. 't Hooft, Nucl. Phys. **B75** (1974) 461
- [22] E. Witten, Nucl. Phys. **B160** (1979) 57
- [23] S. Narison, *QCD Sum Rules* (World Scientific, Singapore, 1990)
- [24] E. N. Nikolov, Ph.D. thesis, Ruhr-Universität Bochum, 1995
- [25] M. Goldberger and S. Treiman, Phys. Rev. **110** (1958) 1178
- [26] M. Gell-Mann, R. Oakes, and B. Renner, Phys. Rev. **175** (1968) 2195
- [27] Th. Meissner and K. Goeke, Nucl. Phys. **A524** (1991) 719
- [28] Chr. V. Christov, A. Z. Górski, K. Goeke, and P. V. Pobylitsa, Nucl. Phys. **A592** (1995) 513
- [29] J. Gasser and H. Leutwyler, Phys. Rep. **87** (1982) 77